Materials Transactions, Vol. 46, No. 6 (2005) pp. 1417 to 1424

EXPRESS REGULAR ARTICLE

Erosion and Corrosion Behaviors of ADI Deposited TiN/TiAlN Coatings by Cathodic Arc Evaporation

Cheng-Hsun Hsu, Jung-Kai Lu, Kuei-Liang Lai and Ming-Li Chen

Department of Materials Engineering, Tatung University, Taipei, 104 Taiwan, R. O. China

Austempered ductile iron (ADI) is a heat-treated ductile iron with acicular ferrite and high-carbon austenite as the matrix of the microstructure. The purpose of this research is to investigate the influence of different hard coatings (PVD-TiN and PVD-TiAlN) on the erosion and corrosion properties of ADI. Also, the coating structure and property were analyzed by using XRD, Rockwell C tester and SEM. The results showed that TiN and TiAlN films identified by XRD could be well deposited on the ADI substrate by the PVD method of cathodic arc evaporation (CAE). Adhesion between coating-layer and ADI substrate was better than that between coating-layer and DI substrate. It was found that the initial source of coated layer peeled for the both substrates occurred at the graphitic sites. The depositing rate of TiAlN was rapider than that of TiN, but it also resulted in the thicker coating thickness and rougher surface for the specimen coated with TiAlN film. After slurry erosion test, the result revealed that erosion resistance of coated specimens was better than that of uncoated specimen. In 3.5 mass% NaCl aqueous for polarization curve test, corrosion current of TiAlN film was smaller than that of TiN film. In 10 vol% HCl solution for immersion test, both TiN and TiAlN coatings could raise the corrosion resistance for ADI material.

(Received February 21, 2005; Accepted May 6, 2005; Published June 15, 2005)

Keywords: *austempered ductile iron, cathodic arc evaporation, TiN, TiAlN, erosion wear, corrosion*

1. Introduction

Since development in 1948, the ductile iron (DI), which possesses excellent mechanical properties and good castability, has been widely applied in many industrial fields where the material often exposed to erosion wear of solid particles and corrosion of acidic or alkaline solutions, such as in piping and hydraulic valve. The erosion and corrosion problems often affect the efficiency and control accuracy in many facilities. Austempered ductile iron (ADI)[1] is a new ferrous material made from ductile iron with austempered heat treatment, and possesses many advantages such as low cost, high strength, good toughness, vibration resistance, wear resistance and fatigue resistance, etc. Thus, ADI has gradually instead of the partial applications of gray cast iron, malleable iron and cast steel in the fields of transportation tools in quarrying and mining industries, gear and bearing of automobile industry.[2] Lots of case hardening methods,[3–6] for example, carburizing, nitriding, carbonitriding and chemical vapor deposition (CVD), are customarily selected to treat metallic material for modifying its mechanical and corrosion properties. However, it is a pity that these case hardening processes are not available to treat ADI. The main cause is that austempering is usually carried out isothermally at the temperatures between Ms and 723 K, while the above conventional processing temperature is too high (up to 1273 K or so) to improve ADI due to higher temperature effect resulting in the microstructure changed and the property deteriorated.

One effective means to overcome this disadvantage is to utilize physical vapor deposition (PVD) technology and coat the material's surface with a thin and dense layer of various films.[7,8] PVD generally refers to three generic coating types that involve evaporation, ion plating, and sputtering. Applying these PVD coating methods with lower processing temperature, almost any solid film may be deposited onto the surface of any metallic material. For instance, in previous work,[9–11] some coatings such as DLC, CrN, TiN, and TiCN, have been successfully synthesized by PVD sputtering process to improve material's fatigue strength and corrosion resistance. Also, Jeongs[12] studied about TiN coated on the surface of DI which had treated by ionitriding prior, however, the ionitriding temperature was over temperature limitation of austempered heat treatment.

Thus, for comparison with ADI in this study, TiN and TiAlN films were respectively deposited on the surface of DI and ADI materials by cathodic arc evaporation (CAE) and further explored the effects of both the coatings on erosion and corrosion behaviors of DI and ADI materials. Analyses of the resulting films were also performed for correlating the erosion and corrosion properties attained to the coating characteristics.

2. Experimental Procedures

2.1 Substrate preparation

The experimental ductile iron (DI) was poured into Y-block casting by a regular foundry practice. The chemical composition of the resulting irons is listed in Table 1. According to the previous studies,[13–15] a single austempering temperature of 633 K was adopted in order to obtain ADI material in this work. The heat-treating procedures were as the following descriptions: (1) preheating at 823 K for 15 minutes, (2) austenitizing at 1173 K for 1.5 hours, then, (3) quenched in a salt bath of 633 K for 2 hours, and finally, (4) air-cooled to room temperature. The schematic heat-treating process is further depicted in Fig. 1.

2.2 Specimens and coating treatment

For erosion testing, the specimen was cut and machined from the above castings to be 35 mm × 35 mm × 5 mm in

Table 1 Chemical composition of the resulting material.

Element	C	Si	Mn	P	S	Mg	Fe
mass%	3.56	2.83	0.22	0.039	0.008	0.042	Bal.

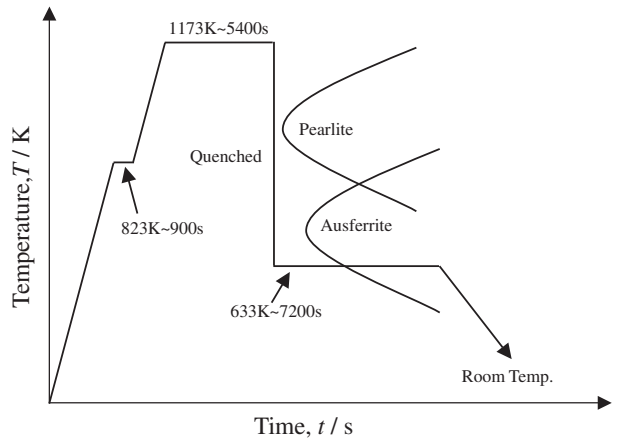

Fig. 1 The schematic of heat-treatment process of austempered ductile iron in this experiment.

size, and also the specimen size of 1.5 mm × 1.5 mm × 5 mm was used for both polarization curve and immersion tests. All the specimens were polished to the same surface roughness (Ra = 0.4 μm) and then cleaned in ultrasonic bath with acetone before dried by hot air. For CAE coating processes, both targets of titanium (99.9%) metal and 50%Ti–50%Al alloy were respectively used to deposit TiN and TiAlN coatings. Prior to deposition, the vacuum chamber was pumped down to 6.7×10^{-3} Pa, and ion bombarded at the bias of −1000 V for 10 minutes was used to clean the surface of substrates (DI and ADI). The detail conditions of coating parameters are listed in Table 2.

Table 2 Coating parameters of TiN and TiAlN films in the experiment.

Film	TiN	TiAlN
Target	Ti	50%Ti–50%Al
Deposition current	70 A	
Substrate bias	−150 V	
Temperature	543~573 K	
Reactive gas	N_2	
Working pressure	2.7×10^{-1} Pa	
Deposition time	30 min	
Thickness	3 μm	6 μm

2.3 Microstructure and film analysis

Optical microscope (OM) was used to observe micro-

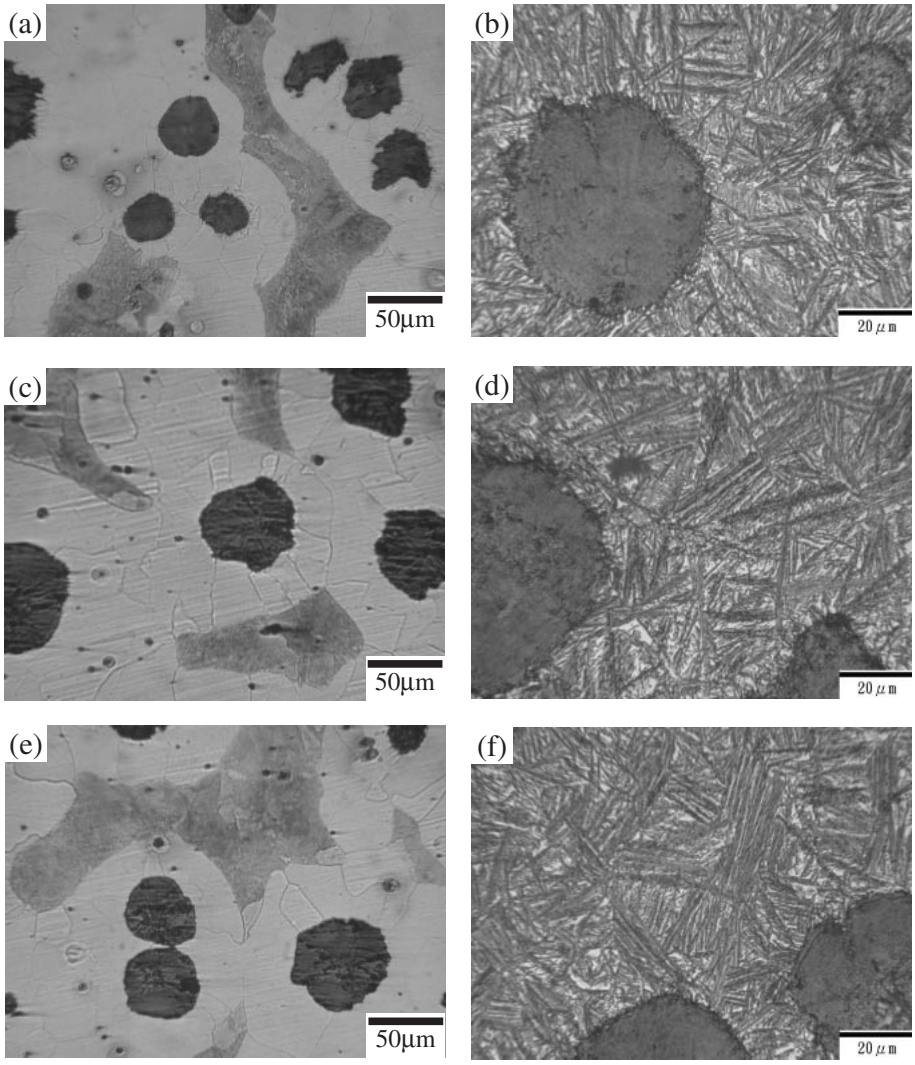

Fig. 2 Microstructure of experimental substrate (a) uncoated DI, (b) uncoated ADI, (c) DI-TiN, (d) ADI-TiN, (e) DI-TiAlN, (f) ADI-TiAlN.

structures of the substrates before and after CAE coating treatments. Crystal structures of the coatings were identified using a Rigaku D/MAX-3A X-ray diffractometer with Cu Kα radiation at 40 kV and 20 mA. A profilometer Surfacorder analyzer (model AY-41) was used to measure the surface roughness (Ra value) of the coated and uncoated specimens. Micro hardness tests were also carried out in Akashi Vickers microhardness tester with a load of 0.49 N. Five hardness readings were taken and averaged to represent the Hv value of the film hardness. Also, the adhesion between film and substrate was evaluated by using a Rockwell hardness C scale indenter. The surface morphology and cross-section of coatings were observed by using scanning electron microscope (SEM).

2.4 Erosion and corrosion tests

The slurry erosion test was adopted to evaluate the behaviors of erosion wear in DI and ADI. The normal incident angle of $\pi/2$ was fixed and water mixed with angular SiO_2 particles about 40–50 μm in averaged size was selected as the eroding carriers. In addition, corrosion current (Icorr.) obtained from the polarization curve in an experimental potentiostatic anodic polarization method is used to evaluate chemical corrosion resistance of the irons. That is, the uncoated and coated specimens were placed in a Nichia model NP-G1001ED apparatus using corrosive media of 3.5 mass% NaCl aqueous solution. Likewise, for immersion test, the uncoated and coated specimens were cleaned by using ultrasonic cleaning with alcohol before immersed in 10 vol% HCl solution at room temperature. The mass loss was measured by using a micro-balance ($\pm 1 \times 10^{-4}$ g) at various time intervals.

3. Results and Discussions

3.1 Microstructure and Coating characteristics

Figure 2 shows the microstructures of uncoated and coated substrates, respectively. The result showed that the microstructures of DI and ADI were almost unchanged after CAE coating treatments controlled in the processing temperature of 543–573 K in this experiment. It implied that both the surface coatings, TiN and TiAlN, were respectively coated onto the DI and ADI substrates, nearly had no detrimental effect on their microstructures. Figure 3 respectively shows

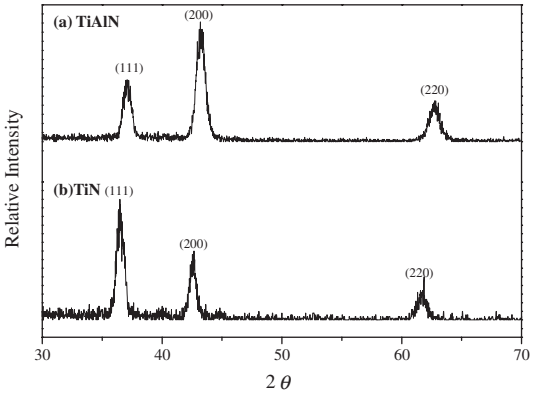

Fig. 3 XRD pattern of (a) TiAlN (b) TiN.

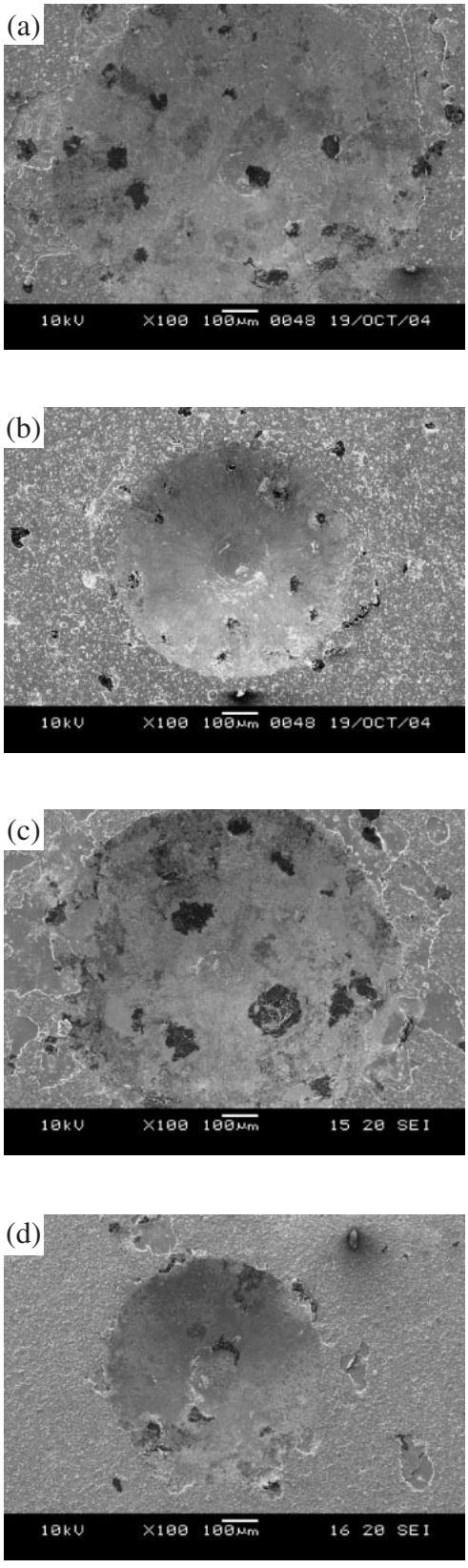

Fig. 4 Fracture morphology of coated specimens by Rockwell C tester (a) DI-TiN, (b) ADI-TiN, (c) DI-TiAlN, (d) ADI-TiAlN.

the X-ray diffraction (XRD) patterns of TiN and TiAlN films in this experiment. It can be found that both of them had the similar orientation peaks but seemed to have a slightly right shift in diffraction angle in TiAlN. According to the study of

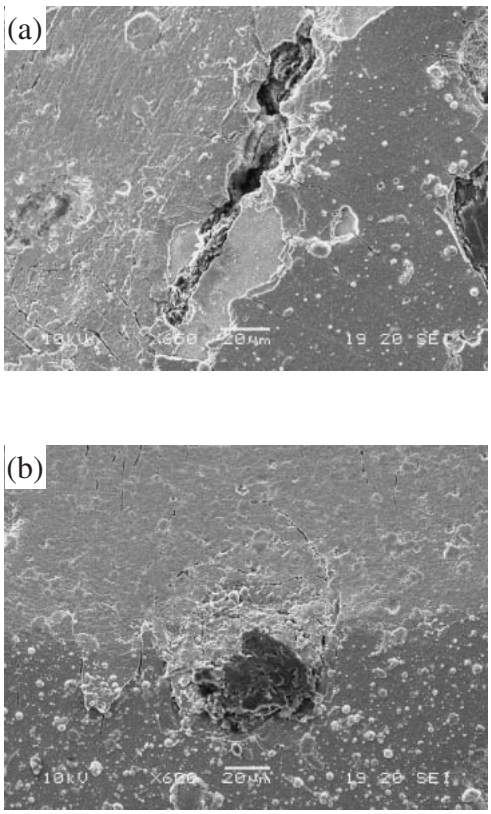

Fig. 5 Peeled film occurred at the graphite sites of coated specimen (a) TiN, (b) TiAlN.

Jones,[16] the strong (111) preferred orientation had been commonly observed from the TiN film deposited by PVD technologies. Another, according to the description of Pinkas,[9] TiAlN coating layer showed relatively multiple orientations mainly of (200) lattice plane. Thus the matter is attributed the changes of crystallographic orientation were caused by the addition of Al element. According to the references,[17–21] the wurtzite structure of AlN was found in TiAlN film if Al over than 65 at%. Besides TiAlN film deposited by the target of Ti/Al (50/50 atomic ratio) no matter sputtering or arc system was only NaCl structure. The target of Ti/Al used for TiAlN film deposited was 50/50 atomic ratio in this study, consequently only NaCl-type TiAlN peaks were identified in the XRD pattern.

Figure 4 presents the indentation marks of coated specimens tested by Rockwell hardness C scale indenter. It is obviously seen that DI substrate coated with TiN and TiAlN films presented large peelings occur in the vicinity of the indentation marks. In contrast, ADI substrate coated regardless of TiN or TiAlN, seemed to have the better adhesion between substrate and the films due to slightly damaged appearance around the indentation marks. The different extent in indented mark was primarily attributed to depend on the hardness of substrate. The ADI substrate with higher hardness, thus its indented mark is smaller than DI substrate with lower hardness. In addition, it was noted that some black spots appeared in the vicinity of indentation marks. It was identified to be the graphitic sites by SEM observation. There is a sharp hardness gradient between graphite and the coatings because the hardness of graphite is quite low

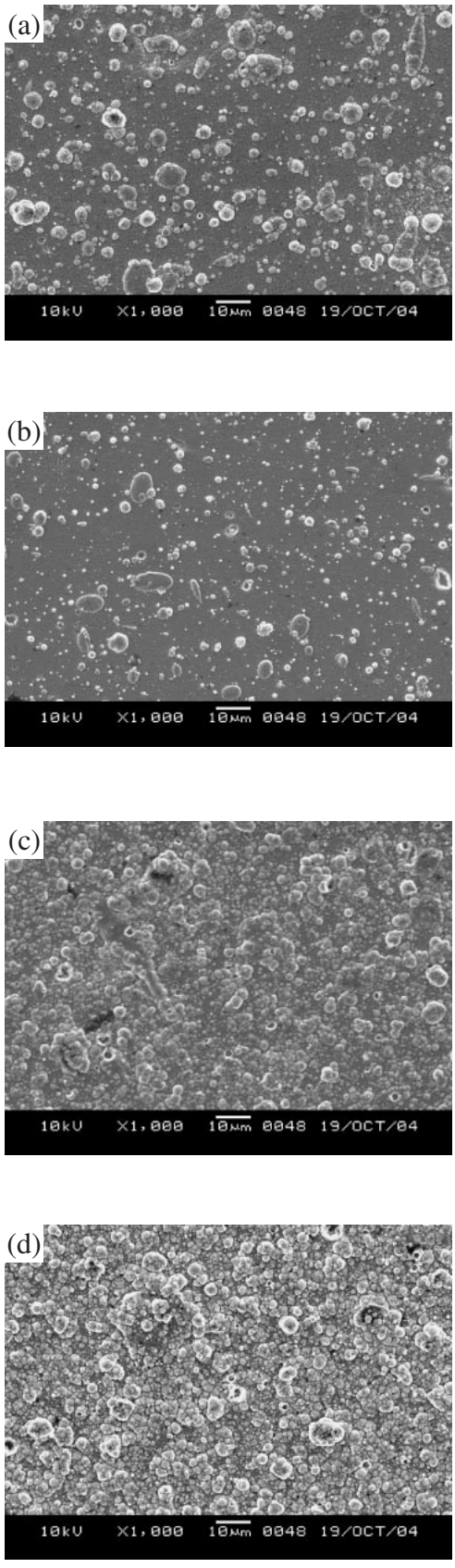

Fig. 6 Surface morphology of coated specimens (a) DI-TiN, (b) ADI-TiN, (c) DI-TiAlN, (d) ADI-TiAlN.

comparable to the ceramic film. Whereupon, the position of interface between nodular graphite and coatings behaved the poor adhesion and the initial source of thin films peeled and

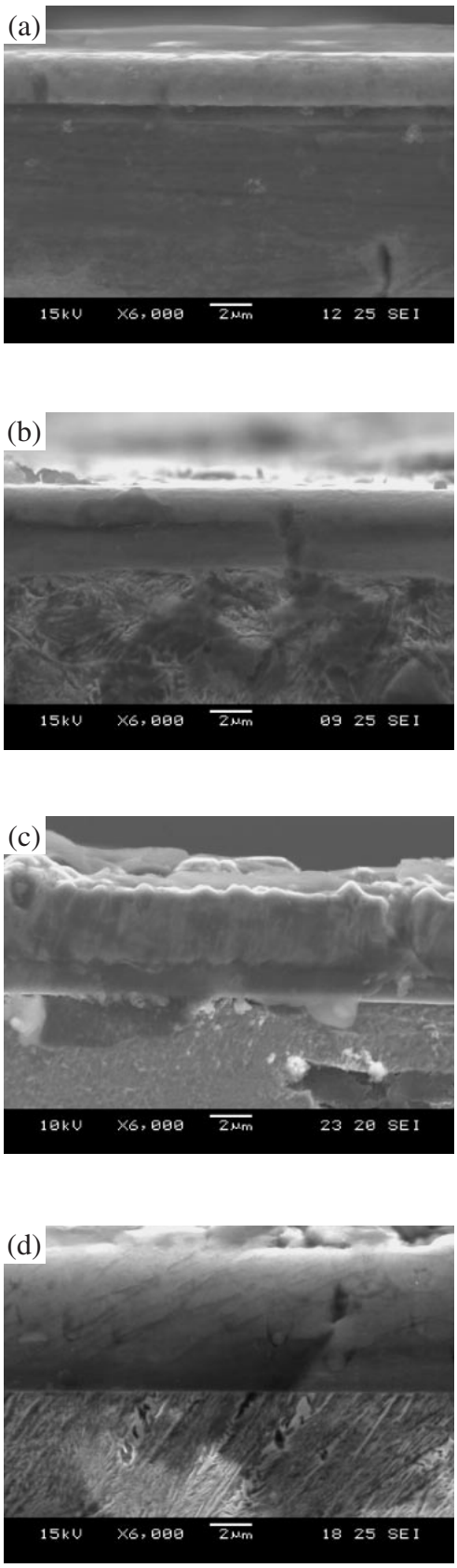

Fig. 7 Cross-sectional view of coated specimens (a) DI-TiN, (b) ADI-TiN, (c) DI-TiAlN, (d) ADI-TiAlN.

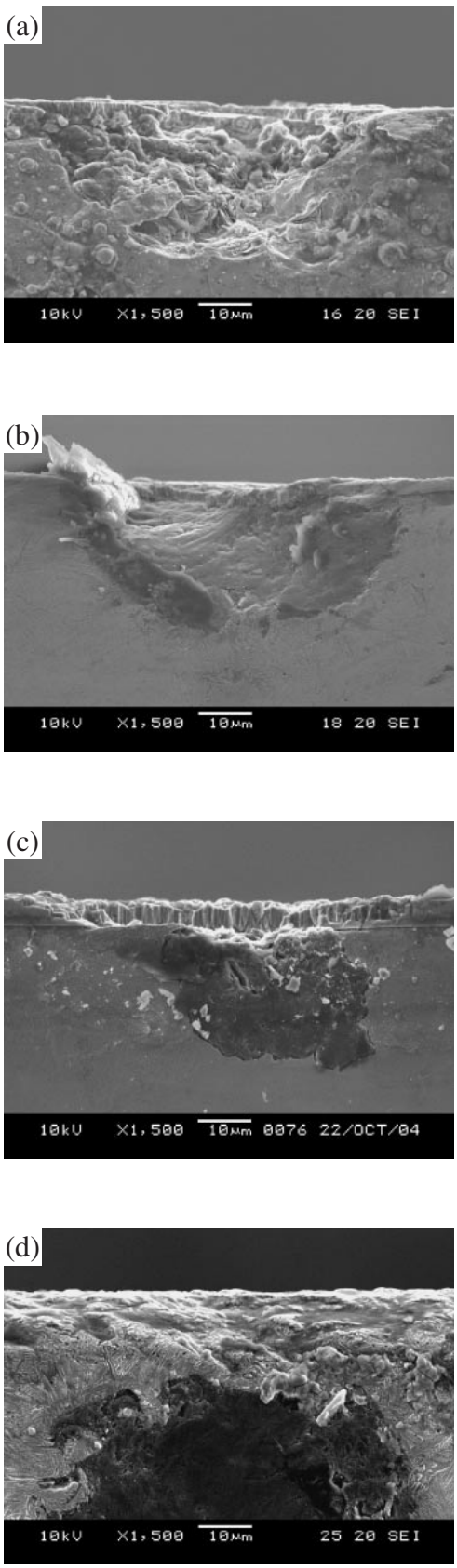

Fig. 8 Eroded cross-sectional morphology of coated specimens (a) DI-TiN, (b) ADI-TiN, (c) DI-TiAlN, (d) ADI-TiAlN.

crack generated, as shown in Fig. 5.

The surface morphologies of coated specimens are presented in Fig. 6. It can be seen that both TiN and TiAlN coatings revealed marco-particle morphology on the surface of DI and ADI substrates. Moreover, TiAlN film seemed to have a rougher surface than TiN film. So this result as

reported by Kourtevs[10] was a kind of characteristics of coating using CAE process. According to SEM observation of cross-section of coated specimen, as shown in Fig. 7, the different thickness of TiN (3 μm) and TiAlN (6 μm) films obtained, respectively, under the same deposition conditions (Table 2) mainly depended on the depositing rate. The depositing rate of TiAlN film is approximately two times compared to TiN film; however, Ra value of TiAlN film is rougher than that of TiN film (0.58–0.59 μm *vs.* 0.36–0.37 μm).

3.2 Coating effect on erosion behavior

The work on dry erosion test of metallic block materials has been performed well in our previous studies.[22,23] But, it is pity that the analogous work is difficult to quantify eroded phenomenon of coatings because the weight loss of thin films was too tiny to measure. Hence the SEM observation of coated specimens after slurry erosion testing was directly utilized to evaluate the erosive behaviors of coated specimens on DI and ADI materials in this study. After 15 minutes erosion testing, both substrates of DI and ADI, eroded surface of the specimens coated with TiN seemed to be more damageable than that coated with TiAlN as shown in Fig. 8. That is, specimen coated TiAlN film was relatively able to prevent nodular graphite peeled from the matrix of DI or ADI compared to that coated TiN film. This result could be attributed to the duplex effect of thickness and hardness of film because thickness and hardness of TiAlN is higher than that of TiN (Thickness: 6 μm *vs.* 3 μm, $Hv_{(0.49\,N)}$: 1700∼1900 *vs.* 1200∼1400). Further compared the substrates of DI and ADI with TiAlN film, it was found ADI substrate presented the more predominant resistant erosion behavior than DI substrate due to occurrence of cracks in the interface between graphite and matrix of DI after erosion testing. Specimens without coatings, also, presented the more severe fracture on the eroded surface after the same erosive conditions. Thus the ADI specimen with TiAlN coating in 6 μm thickness showed the best slurry erosion resistance while uncoated specimens got the worse performance.

3.3 Coating effect on corrosion behavior

Polarization curves of all specimens after polarization test in 3.5 mass% NaCl aqueous solution are showed in Fig. 9 and the corrosion current (Icorr.) obtained is listed at Table 3, respectively. From comparison of the result, it can be found uncoated ADI had better corrosion resistance in NaCl solution than un-coated DI material. The main reason is that ADI possesses the specific microstructure containing the

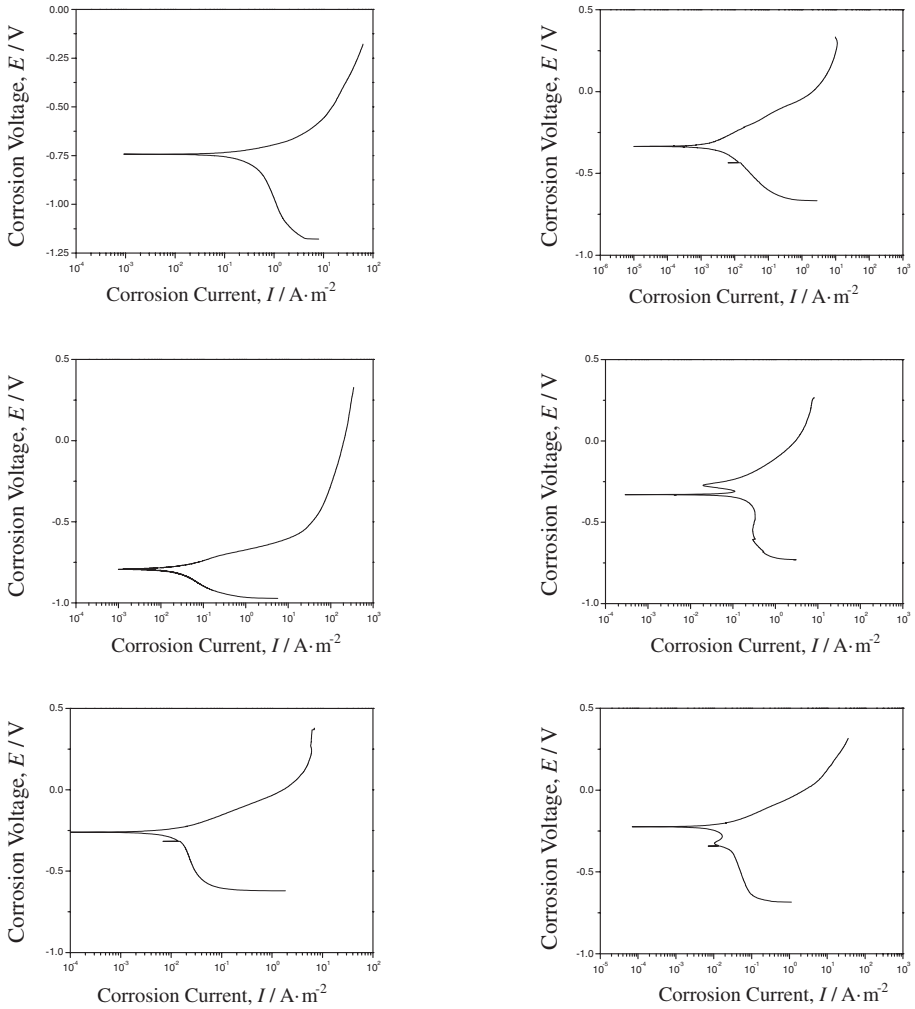

Fig. 9 The polarization curves of uncoated and coated specimens in 3.5 vol.% NaCl aqueous solution (a) DI (b) ADI (c) DI-TiN (d) ADI-TiN (e) DI-TiAlN (f) ADI-TiAlN.

Table 3 Surface roughness, microhardness and polarization current of the uncoated and coated specimens in this experiment.

Materials	Ra value (μm)	Microhardness $(Hv)_{0.49N}$	Icorr (1×10^{-3} A/m^2)
DI	0.4	195	378.43
ADI	0.4	400	129.37
DI-TiN	0.36	1200	25.73
ADI-TiN	0.37	1400	20.98
DI-TiAlN	0.58	1700	16.19
ADI-TiAlN	0.59	1900	2.94

retained austenite and dense ausferrite. Further, specimens coated with TiAlN or TiN film could provide a protective surface layer to improve the corrosion resistance of DI and ADI materials due to the passivation effect resulting from formation of passive films such as aluminum or titanium oxide. In particular ADI coated with TiAlN showed the best corrosion resistance in 3.5 mass% NaCl aqueous solution.

On the other hand, immersion test was carried out to determine the corrosion weight loss and corrosion rate at room temperature. The results for all specimens immersed in 10 vol% HCl solution are showed in Fig. 10. It obviously revealed that uncoated DI had the worst performance on corrosion resistance in 10 vol% HCl solution, and then was uncoated ADI subsequently. For all coated specimens immersed in 10 vol% HCl solution, they preferably showed

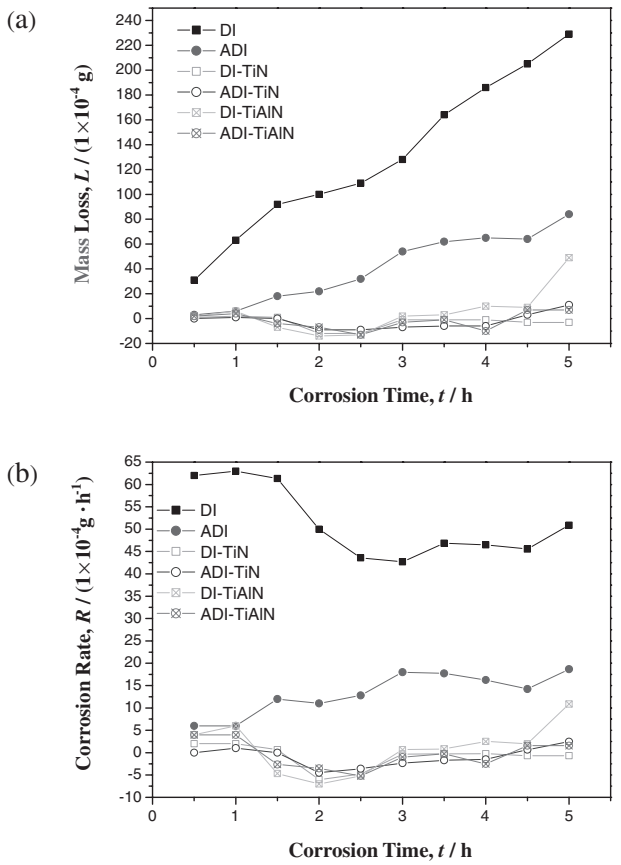

Fig. 10 Weight loss and corrosion rate of the various specimens immersed in 10% HCl aqueous solution.

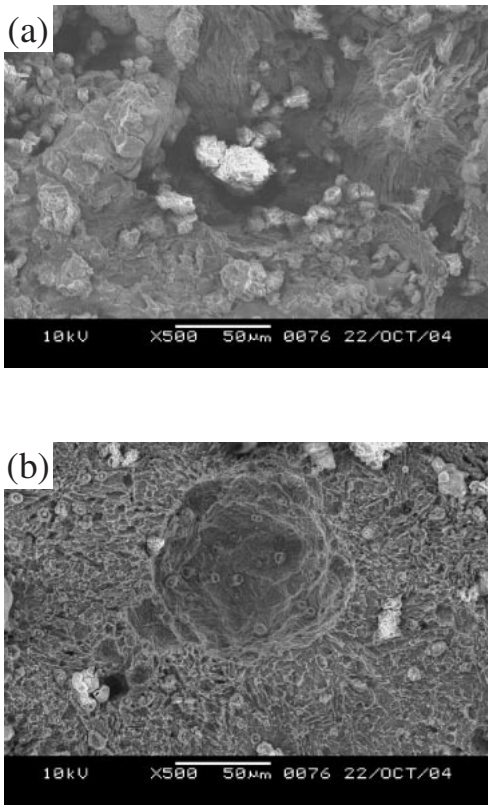

Fig. 11 Surface morphology of uncoated specimens after immersed in 10% HCl aqueous solution (a) DI (b) ADI.

the better corrosion resistance than uncoated specimens did. Similarly, coated specimens revealed a trend that slightly increasing, subsequently decreasing in corrosion rate by means of formation of passive films such as aluminum or titanium oxide first them pitting. Surface morphologies of the uncoated and coated specimens after 5 hours corrosion in 10 vol% HCl are showed in Figs. 11 and 12, respectively. From these SEM photos, it can be clearly seen that the surface of uncoated specimen was severely damaged and presented uniform corrosion morphology. In contrast to coated specimen, only with partial pitting corrosion occurred in the site of nodular graphite on the surface of specimen. And the DI substrate coated specimen was more damageable than that of ADI in 10 vol% HCl solution.

4. Conclusion

In this work, TiN and TiAlN thin films could be successfully deposited on both substrates of DI and ADI by the method of PVD-CAE system. In particular, these films coated on ADI substrate revealed better adhesion than DI substrate because of less on hardness gradient between coated layer and substrate. However, it was also noted that nodular graphite in the matrix was an initial source for films peeled. At the same coating parameters, TiAlN had the faster depositing rate than TiN but showed rougher surface, simultaneously. For slurry erosion test, the result revealed that erosion resistance of coated specimens was better than that of uncoated specimen and TiAlN revealed better erosion resistance than TiN due to the effect of hardness. For

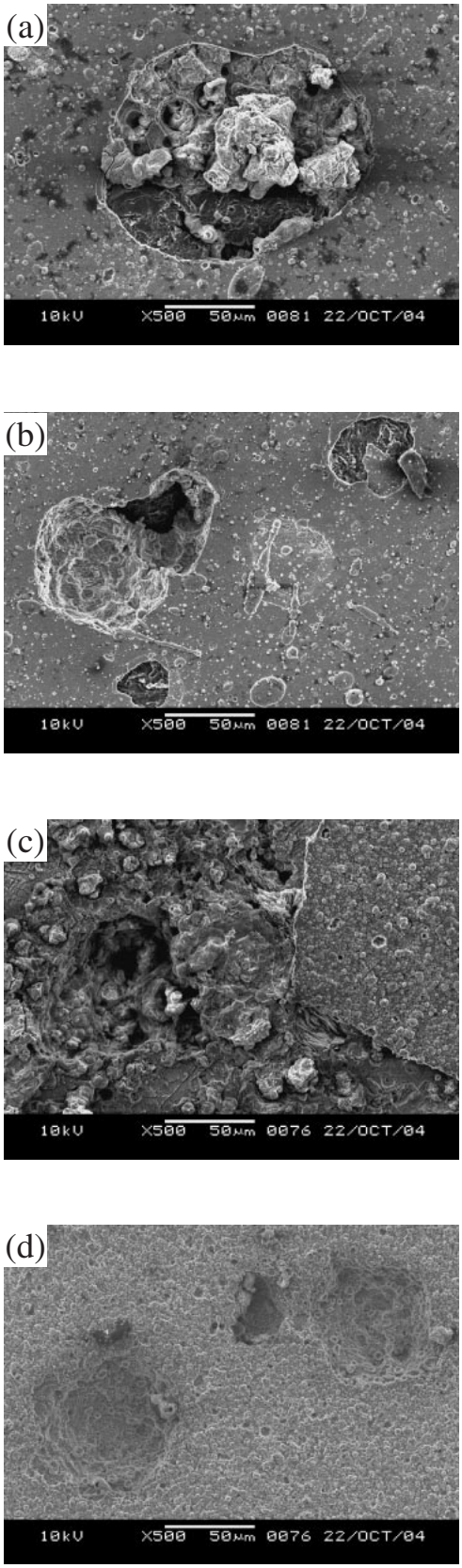

Fig. 12 Surface morphology of coated specimens after immersed in 10% HCl aqueous solution (a) DI-TiN, (b) ADI-TiN, (c) DI-TiAlN, (d) ADI-TiAlN.

polarization curve test in 3.5 mass% NaCl aqueous, ADI showed better performance than DI because the specific microstructure of ADI containing retained austenite and dense ausferrite. In addition, corrosion current of TiAlN film was smaller than that of TiN film by means of aluminum oxide formed. For immersion test in 10 vol% HCl aqueous, both TiN and TiAlN coatings revealed a trend that slightly increasing, subsequently decreasing in corrosion rate by means of formation of passive films such as aluminum or titanium oxide first them pitting.

Acknowledgements

The authors wish to thank the financial support of the National Science Council (Taiwan) under project No. NSC93-2216-E-036-015.

REFERENCES

1) K. Hornung: Heat Treatment of Metals **4** (1986) 87–94.
2) S. K. Putatunda: Mater. Sci. Eng. A **315** (2001) 70–80.
3) D. Dragomir and L. Druga: Mater. Sci. Eng. A **302** (2001) 115–119.
4) M. Okumiya, Y. Tsunekawa and T. Murayama: Surf. Coatings Technol. **142–144** (2001) 235–240.
5) S. Charizanova, G. Dimitrov, E. Rousseva and V. Marcov: Journal of Materials Processing Technology **77** (1998) 73–79.
6) O. H. Kessler, F. T. Hoffmann and P. Mayr: Surf. Coatings Technol. **120–121** (1999) 366–372.
7) H. P. Feng, S. C. Lee, C. H. Hsu and J. H. Ho: Materials Chemistry and Physics **59** (1999) 154–161.
8) M. I. Jones, I. R. McColl and D. M. Grant: Surf. Coatings Technol. **132** (2000) 143–151.
9) M. Pinkas, J. Pelleg and M. P. Dariel: Thin solid films, **355–356** (1999) 380–384.
10) J. Kourtev, R. Pascova and E. Weibmantel: Thin solid films, **287** (1996) 202–207.
11) H. P. Feng, C. H. Hsu, J. K. Lu and Y. H. Shy: Mater. Sci. Eng. A **347** (2003) 123–129.
12) J. J. Jeong, B. Y. Jeong, M. H. Kim and C. Lee: Surf. Coatings Technol. **150** (2002) 24–30.
13) C. H. Hsu, S. C. Lee, H. P. Feng and Y. H. Shy: Metall. Mater. Trans. A **32A** (2001) 295–303.
14) C. H. Hsu and T. L. Chuang: Metall. Mater. Trans. A, **32A** (2001) 2509–2514.
15) S. C. Lee, C. H. Hsu, C. C. Chang and H. P. Feng: Metall. Mater. Trans. A **29A** (1998) 2511–2521.
16) M. I. Jones, I. R. McColl and D. M. Grant: Surf. Coatings Technol. **132** (2000) 143–151.
17) Y. Setsuhara, T. Suzuki, Y. Makino, S. Miyake, T. Sakata and H. Mori: Surf. Coatings Technol. **97** (1997) 254–258.
18) H. C. Brashilia, M. S. Prakash, A. Jain and K. S. Rajam: Vacuum **77** (2005) 169–179.
19) A. Horling, L. Hultman, M. Oden, J. Sjolen and L. Karlsson: Surf. Coatings Technol. **191** (2005) 384–392.
20) K. L. Lin, W. H. Chao and C. D. Wu: Surf. Coatings Technol. **89** (1997) 279–284.
21) D. G. Kim, T. Y. Seong and Y. J. Baik: Thin Solid Films **397** (2001) 203–207.
22) C. H. Hsu, S. C. Chiu, J. K. Lu and Y. H. Shin: Mater. Trans. **45** (2004) 577–583.
23) H. Y. Teng, C. H. Hsu, S. C. Chiu and D. C. Wen: Mater. Trans. **44** (2003) 1480–1487.